Predicting the Formation of Mud Cracks in Li-ion Battery Electrodes During the Drying Process with In Situ X-ray Computed Tomography: Supplementary Information

Will J. Dawson,[1,2,3] Andrew R.T. Morrison*[2,3], Simon M. Tonge[3,7], Matthew P. Jones[2], Kofi Coke[2,3,10], Isabel C. Antony[2,3,4,5,6], Kaz Wanelik[4], Vyacheslav Kachkanov[4], Partha P. Paul[7,11], Bratislav Lukić[7,8], Robert Scott Young[2], Zifa Zuhair[2,4], James Parker[3,9], Inez Kesuma[2,6], Gargi Giri[2,3,6], Liam Bird[2,3,6], Alexander J. E. Rettie[1,2], Rhodri Jervis[1,2,3], James B. Robinson[1,3], Denis Cumming[3,9], Thomas S. Miller[1,2,3], Paul R. Shearing*[3,6]

1. Advanced Propulsion Lab, UCL East, University College London, London, E20 2AE, UK.
2. Electrochemical Innovation Lab, University College London, London, WC1E 7JE, UK.
3. The Faraday Institution, Didcot, OX11 0RA, UK.
4. Diamond Light Source, Harwell Science and Innovation Campus, Didcot, Oxfordshire, OX11 0DE, UK.
5. ISIS Neutron and Muon Source, Rutherford Appleton Laboratory, OX11 0QX Harwell, UK.
6. The ZERO Institute University of Oxford, Holywell House, Osney Mead, Oxford, OX2 0ES.
7. ESRF – The European Synchrotron Radiation Facility, 71 Av. des Martyrs, 38000 Grenoble, France.
8. Institut Max von Laue - Paul Langevin, ILL, 71 Av. des Martyrs, 38000 Grenoble – France.
9. School of Chemical, Materials and Biological Engineering, The University of Sheffield, Sheffield, UK, S1 3JD.
10. School of Chemistry and Chemical Engineering, University of Southampton, Southampton, SO17 1BJ.
11. SLAC National Accelerator Laboratory, Menlo Park, CA 94025-7015

* Corresponding authors

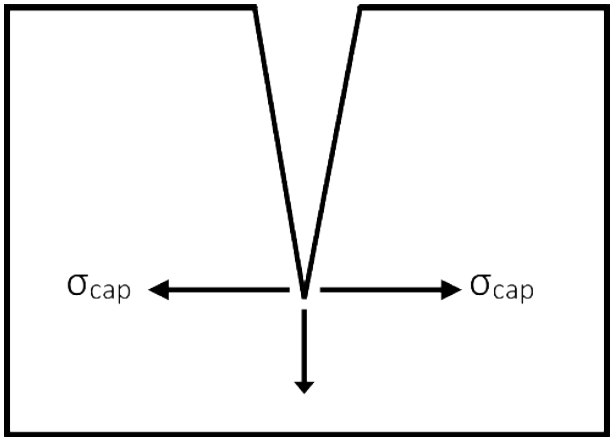

Figure S1 - Diagram showing the direction of crack propagation downwards, perpendicular to the direction of capillary stress, σ_{cap}.

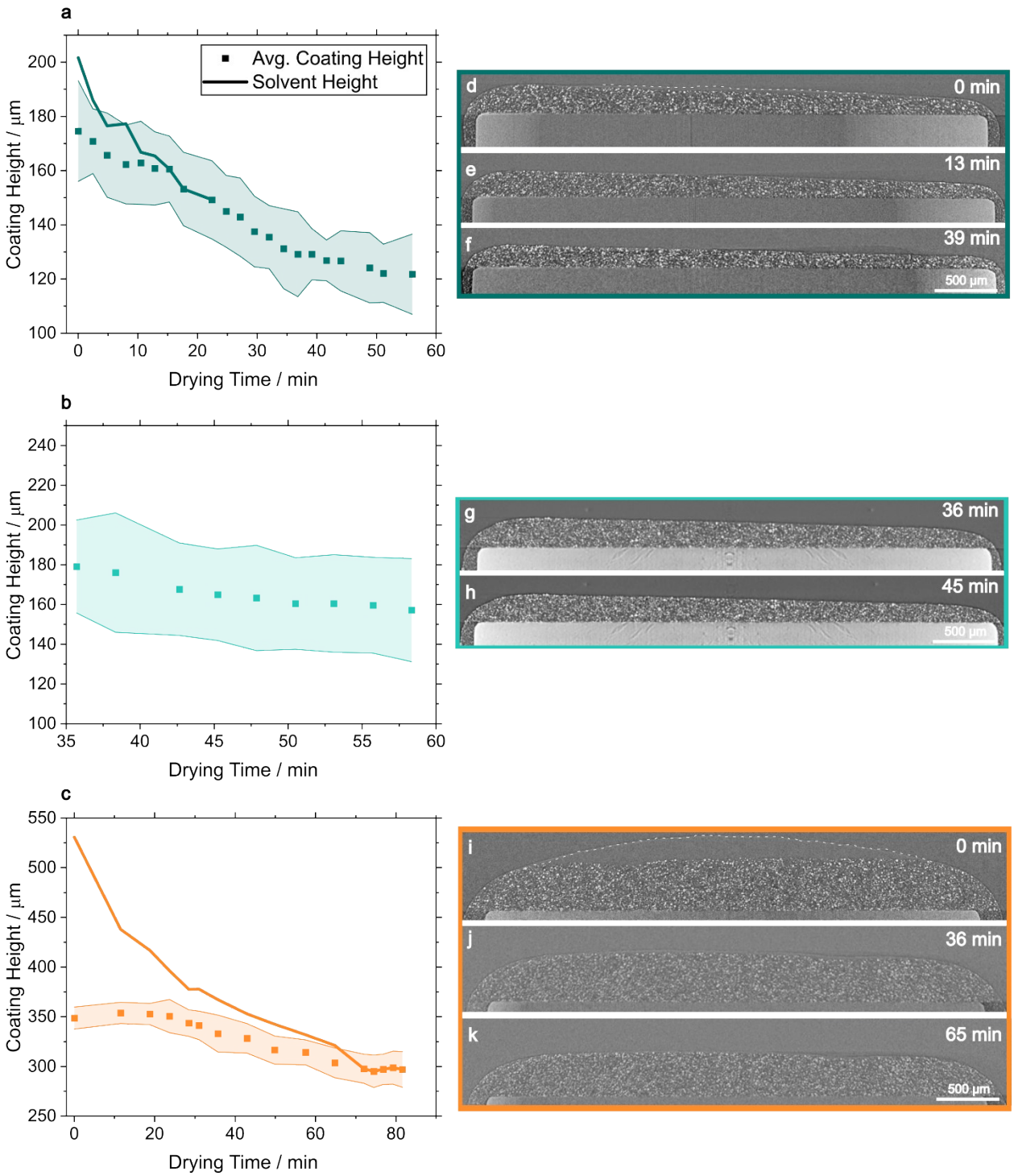

Figure S2 – Plots of coating height vs drying time for each individual coating thickness (a) 300 µm, (b) 500 µm, (c) 800 µm. Solid lines represent the solvent height, where visible above the solid coating layer, and the shaded region shows the standard deviation of average coating height. Central x-z slices from reconstructed X-ray CT volumes are shown adjacent to their corresponding plots in (d-k), where dashed white lines in the 0 minute image for 300 um and 800 um electrodes (d and i respectively) indicate the visible solvent front. Due to partial failures during the imaging process, images of the 500 µm coating drying process before 36 minutes were lost and only the final period of electrode consolidation is shown.

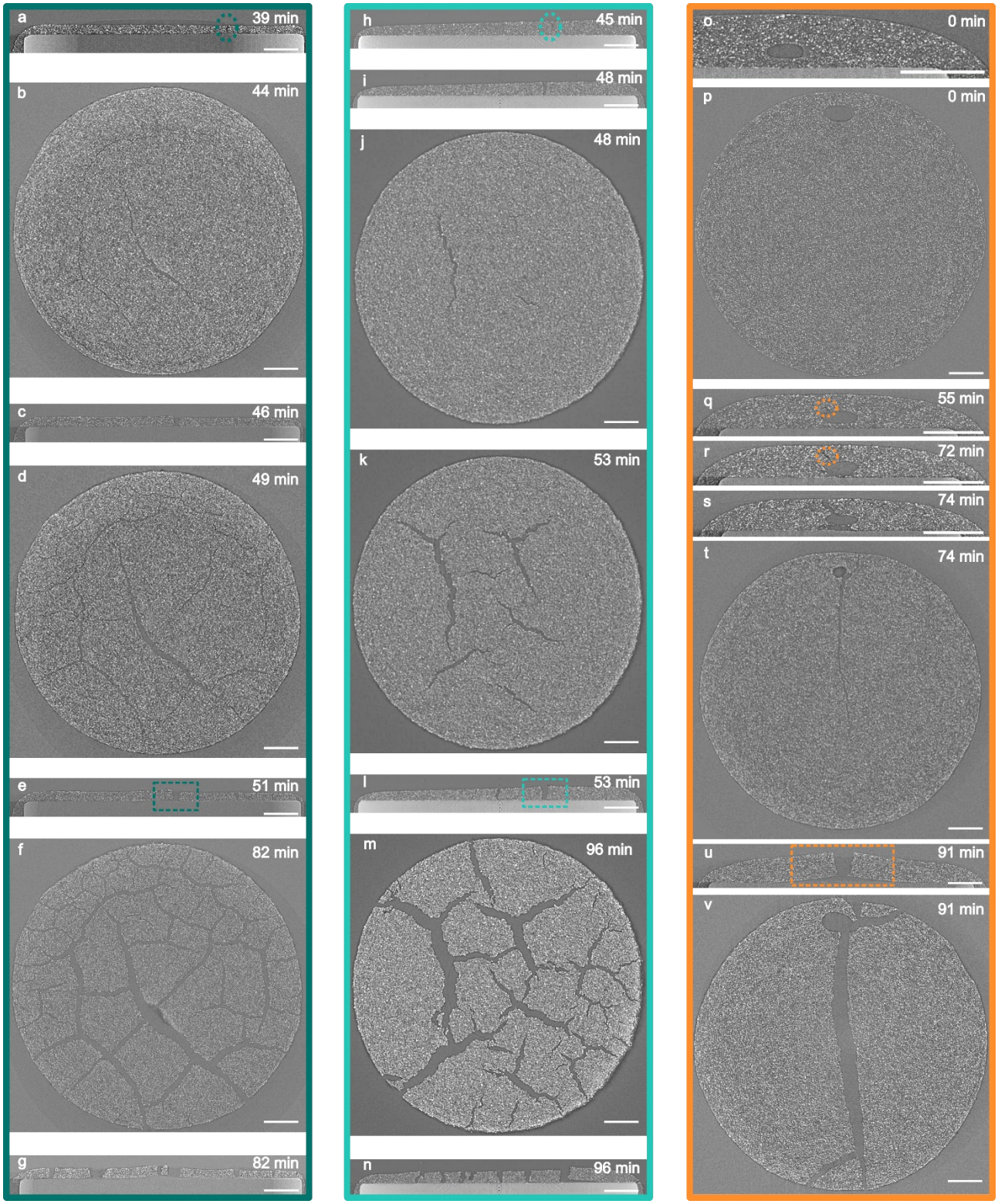

Figure S3 – Series of representative 2D images slices in the x-y and x-z planes showing the initiation and propagation in the 300 µm (a-g), 500 µm (h-n) and 800 µm (o-v) electrodes. Ellipsoid dashed regions (a, h, q, r) indicate positions of has escape from bubbles and crack initiation. Rectangular dashed regions in (e, l, u) indicate positions where cracks act as nucleating points for delamination. All scale bars show 500 µm.

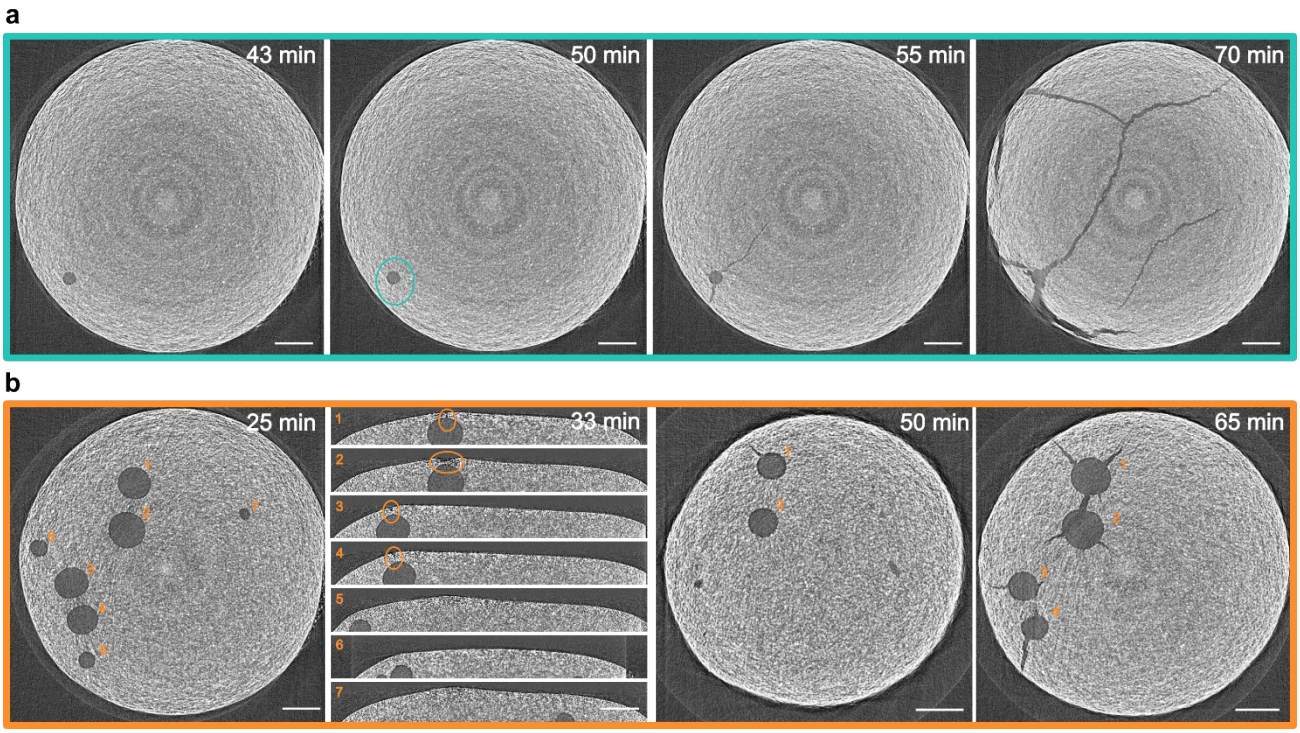

Figure S4 - Two series of slices from X-ray CT reconstructions from imaging at Diamond Light Source showing the growth of cracks when (a) 1 bubble was present and (b) multiple numbered bubbles were present in the slurry. Circled regions indicate the time and position of initial escape of gas from the bubbles. All scale bars represent 500 µm.

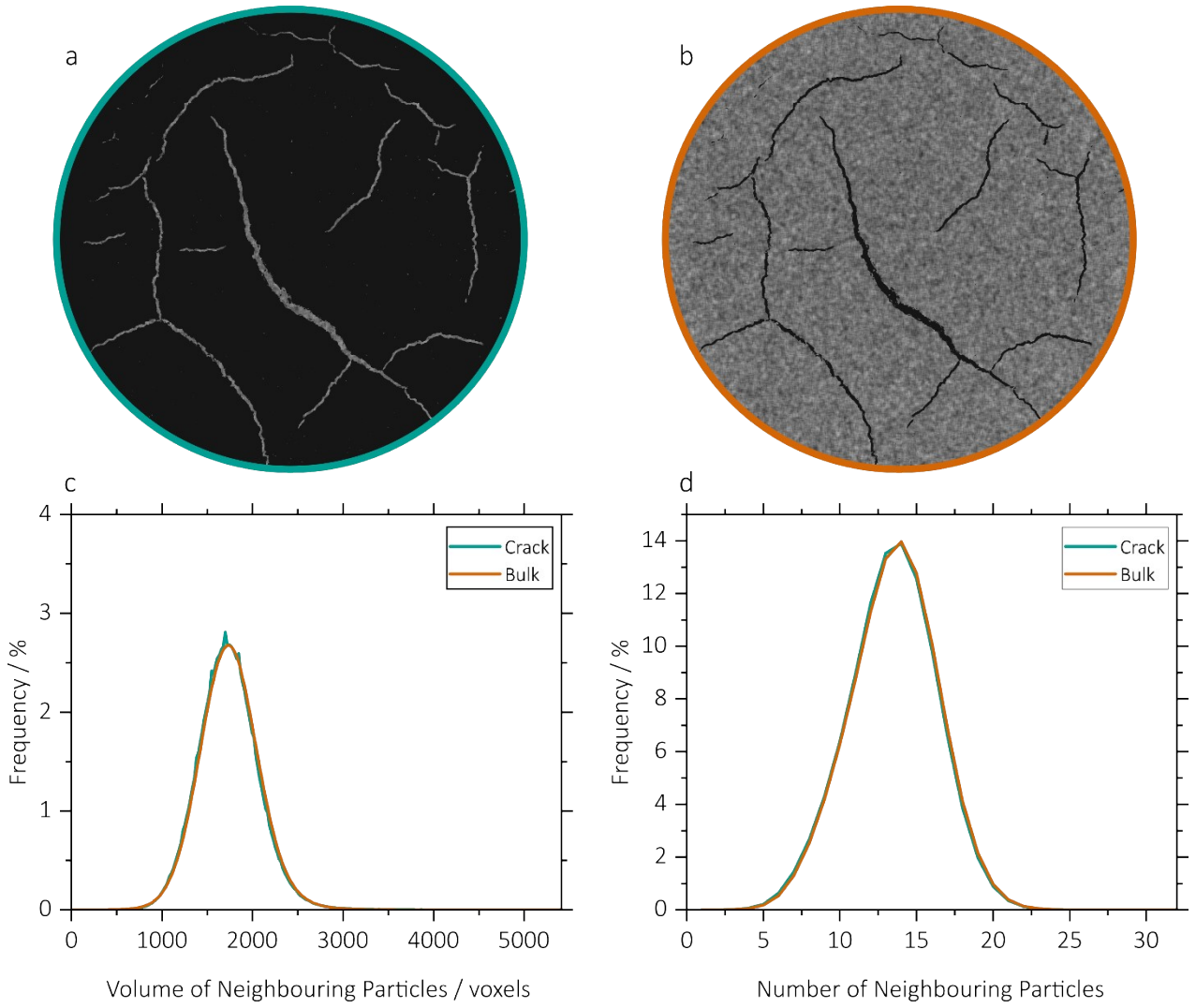

Figure S5 - Analysis of the closeness or particle packing in the 300 µm electrode, where (a) and (b) show the same single slice from the region analysed, indicating the crack region and the bulk region respectively; (c) shows the distribution of volume of particles in neighbouring voxels within these two regions and (b) shows the number of neighbouring particles for each voxel in these two regions.

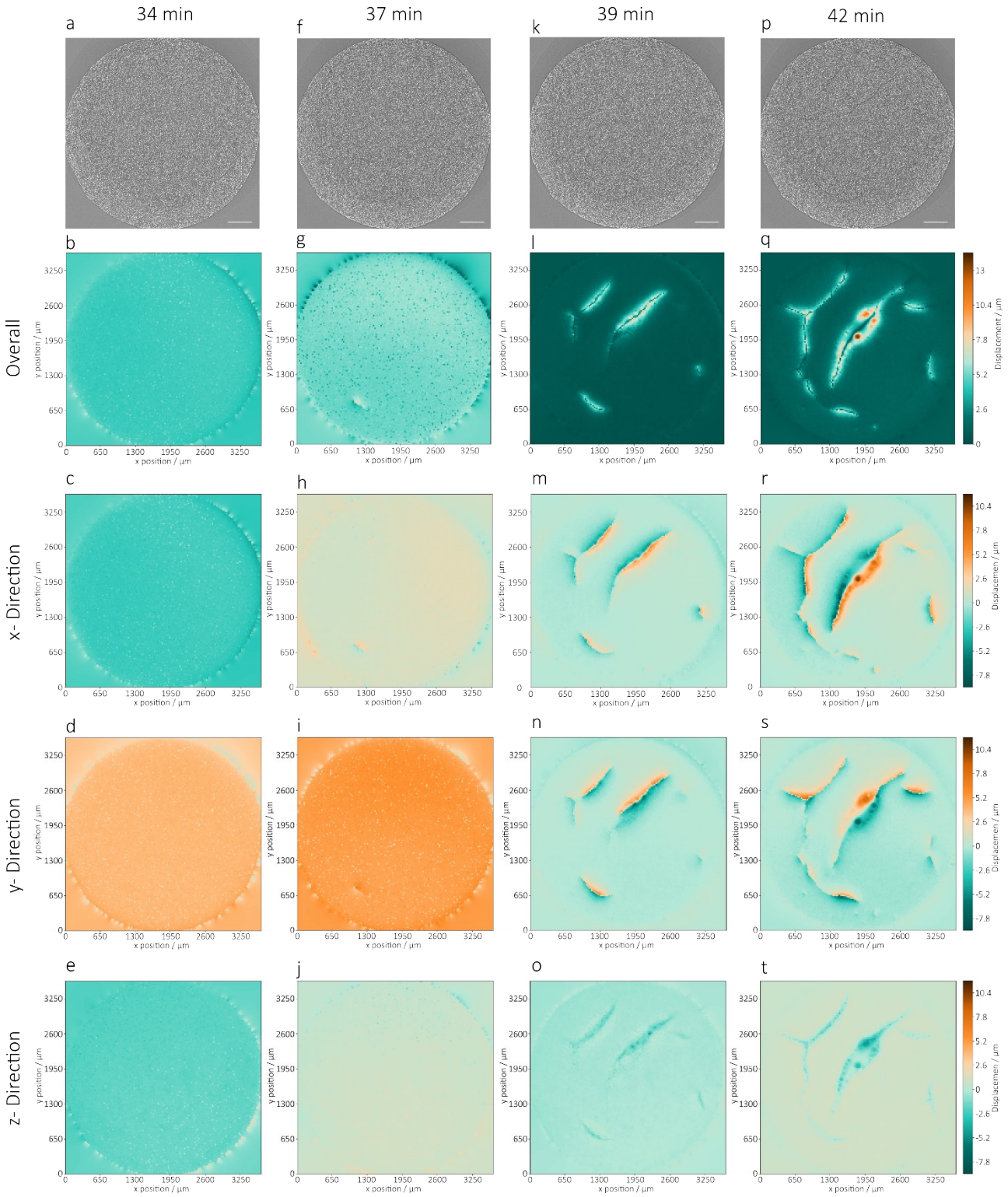

Figure S6 – Representative single slices from four time steps analysed with DVC for three X-ray CT images for the 300 µm electrode, from 34 to 42 minutes of drying time. A raw reconstructed central slice is shown for each time step (a, f, k, p), alongside maps of overall displacement (b, g, l, q) and displacement in the x- (c, h, m, r), y- (d, i, n, s) and z-directions (e, j, o, t).

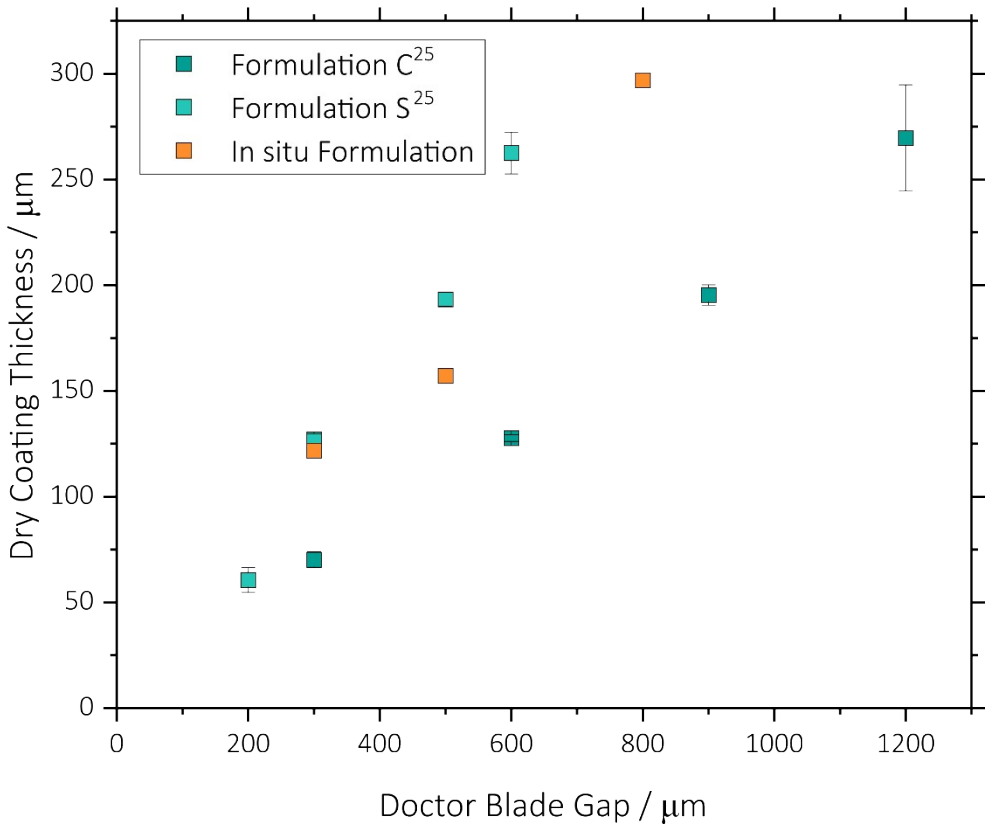

Figure S7 - Plot showing the relationship between coating blade wet gap and dry coating thickness for two formulations tested in bulk electrodes, taken from previous work, and the present formulation used in situ on 4mm pins.[25]